Blind Source Separation in document restoration: an interference level estimation

A. Boccuto, I. Gerace and V. Giorgetti *

Abstract

We deal with the problem of blind separation of the components, in particular for documents corrupted by bleed-through and show-through. So, we analyze a regularization technique, which estimates the original sources, the interference levels and the blur operators. We treat the estimate of the interference levels, given the original sources and the blur operators. In particular, we investigate several GNC-type algorithms for minimizing the energy function. In the experimental results, we find which algorithm gives more precise estimates of the interference levels.

1 Introduction

In this paper we deal with a *Blind Source Separation* (BSS) problem. These topics have been widely studied since the end of the last century, and have various applications.

In particular, we analyze the digital reconstruction of degraded documents. We observe that weathering, powder, humidity, seeping of ink, mold and light transmission can determine the degradation of the paper and the ink of written text. Some of the consequences in damaged documents are, for instance, stains, noise, transparency of writing on the verso side and on the close pages, unfocused or overlapping characters, and so on. Historically, the first techniques of restoration for degraded documents were manual, and they led to a material restoration. Recently, thanks to the diffusion of scanners and software for reconstruction of images, videos, texts, photographs and films, several new techniques were used in the recovery and restoration

*Authors' Address: A. Boccuto, I. Gerace : Dipartimento di Matematica e Informatica, via Vanvitelli, 1 I-06123 Perugia, Italy, E-mail: antonio.boccuto@unipg.it, ivan.gerace@unipg.it ; V Giorgetti: Dipartimento di Matematica e Informatica "U. Dini", viale G. B. Morgagni, 67/A 50134 Firenze, Italy, E-mail: valentina.giorgetti@unifi.it

Key words and phrases: Blind source separation, image restoration, document restoration, bleed-through, show-through, GNC technique.

of deteriorated material, like for instance digital or virtual restoration. Digital imaging for documents is very important, because it allows to have digital achieves, to make always possible the accessibility and the readability. The *Digital Document Restoration* consists of a set of processes finalized to the visual and aesthetic improvement of a virtual reconstruction of a corrupted document, without risk of deterioration.

We deal with *show-through* and *bleed-through* effects. The show-through is a front-to-back interference, caused by the transparency of the paper and the scanning process, and by means of which the text in the recto side of the document can appear also in the verso side, and conversely. The bleed-through is an intrinsic front-to-back physical deterioration caused by ink seeping, and its effect is similar to that of show-through. The physical model for the show-through distortion, is very complex, because there are the spreading of light in the paper, the features of the paper, the reflectance of the verso and the transmittance parameters. In [22], Sharma gave a mathematical model was first analyzed and then further approximated so to become easier to handle. This model describes the observed recto and verso images as mixtures of the two uncorrupted texts. A nonlinear modified Sharma model is proposed in [13, 18, 19, 21]. Some nonlinear models which assume that the interference levels depend on the location are presented in [9, 12, 24]. So, the model turns to be non-stationary, that is not translation invariant. The algorithms in [9, 24] for the resolution of the related inverse problem are fast heuristics. In [4], a non-stationary model is proposed. However, in order to obtain more precise results, a computationally more expensive regularized problem has been sketched in [8] and [23]). Now we analyze in detail the iterative technique to solve such a model, in which the sources, the blur operators and the interference level are computed separately at every step, until a fixed point is found. In this paper, in particular, we deal with determining the interference level, by fixing the blur operators and the ideal sources. To this aim, we use a GNC-type technique (see, e.g., [1, 2, 3, 5, 6, 11, 14, 15, 16, 17, 20]). In a forthcoming paper, the steps about finding the blur operators and the ideal sources will be treated.

The paper is structured as follows. In Section 2 we deal with the regularization of the modified Sharma model. In Section 3 we describe the alternating iterative algorithm, used to find the minimum of the energy function. In Section 4 we analyze the technique to determine the interference levels, given the blur operator and the ideal sources. In Section 5 we propose different types of convex approximations. In Section 6 we present GNC-type alternative minimization techniques. In Section 7 we compare the proposed technique by means of the experimental results.

2 Regularization of the problem

In this paper we consider a modified Sharma-type model related to the show-through phenomenon in paper documents, as follows (see, e.g., [8, 23]):

$$\begin{cases} f^s(i,j) = f(i,j)e^{q_r(i,j)\left(\frac{z_r(i,j)}{N}-1\right)} \\ r^s(i,j) = r(i,j)e^{q_f(i,j)\left(\frac{z_f(i,j)}{N}-1\right)} \end{cases}, \tag{1}$$

where N is the maximum value of the light intensity, which is assumed to correspond with the background of the analyzed document; $q_f(i,j)$ is the interference level which affects the light intensity of interferences from the recto to the verso; $q_r(i,j)$ is the interference level which affects the light intensity of interferences from the verso to the recto; $f^s = [f^s(i,j)]_{i=1,\dots,n,j=1,\dots,m}, r^s = [r^s(i,j)]_{i=1,\dots,n,j=1,\dots,m} \in \mathbb{R}^{nm}$ are the vectors which represent the observed mixtures (expressed in the lexicographic form); $f = [f(i,j)]_{i=1,\dots,n,j=1,\dots,m}, r = [r(i,j)]_{i=1,\dots,n,j=1,\dots,m} \in \mathbb{R}^{nm}$ are the vectors which represent the ideal images of the recto and the verso of the document (expressed in the lexicographic form); $z_f = [z_f(i,j)]_{i=1,\dots,n,j=1,\dots,m} = Af, z_r = [z_r(i,j)]_{i=1,\dots,n,j=1,\dots,m} = Ar$ are the blurred images of the recto and the verso, where $A \in \mathbb{R}^{(nm)\times(nm)}$ is the blur operator, which in general has the form of a matrix with Toeplitz blocks.

The problem of the blind separations of components consists of finding an estimate of the recto/verso pair of the source document, which is denoted by $s = (f,r)$, of the interference level $q = (q_f, q_r)$ and of the blur operator A, given in input the observed images of the recto and the verso. This is an ill-posed problem in the Hadamard sense, because in general it can have no solutions, or the solution can be not unique and/or not stable with respect to small variations of the data.

To estimate the solution of the problem, some regularization techniques are used, which substantially consist of finding the minimum of a function, called *energy function*, by imposing some uniformity constraints on the solution.

The solution of the considered problem is

$$(f^*, r^*, q^*, A^*) = \arg \min_{(f,r,q,A)} E(f,r,q,A),$$

where

$$E(f,r,q,A) = T(f,r,q,A) + \widehat{S}(f) + \widehat{S}(r) + S(q_f) + S(q_r) + S_c(q_f,q_r) \tag{2}$$

is the *energy function*, and

$$\begin{aligned} T(f,r,q,A) &= T_f(q_r) + T_r(q_f) = \sum_{i=1}^{n}\sum_{j=1}^{m}\left(f^s(i,j) - f(i,j)\mathrm{e}^{-q_r(i,j)\left(1-\frac{z_r(i,j)}{N}\right)}\right)^2 + \\ &+ \sum_{i=1}^{n}\sum_{j=1}^{m}\left(r^s(i,j) - r(i,j)\mathrm{e}^{-q_f(i,j)\left(1-\frac{z_f(i,j)}{N}\right)}\right)^2 \end{aligned} \tag{3}$$

is the *consistency term*, which measures the faithfulness of the solution to the data, and $\widehat{S}(f) + \widehat{S}(r)$ is the *regularization term*, or *smoothness term*, which is chosen according to the properties which the estimated source has to satisfy, and measures the faithfulness of the estimated source to a priori informations. Moreover, the last terms of (2) are given by

$$S(q_v) = \sum_{i=1}^{n}\sum_{j=1}^{m} \lambda_v^2 \Big(q_v(i,j) - q_v(i-1,j) \Big)^2 + \sum_{i=1}^{n}\sum_{j=1}^{m} \lambda_v^2 \Big(q_v(i,j) - q_v(i,j-1) \Big)^2,$$

where $v \in \{f, r\}$, λ_v is the regularization parameter related to the interference level of the recto (resp. verso), if $v = f$ (resp., $v = r$), and

$$S_c(q_f, q_r) = \sum_{i=1}^{n}\sum_{j=1}^{m} \lambda_c^2 (q_f(i,j) - q_r(i,j))^2$$

is the joint smoothness term. The parameter λ_c is the regularization parameter between the interference of the recto and the verso with respect to the same pixel.

3 Alternating techniques

To minimize the function in (2), we use a strategy of *alternating minimization*, which consists of the estimation of the minimum of the function with respect to each single variable, fixing the other ones. We proceed according the following scheme:

$k = 0$

initialize f_0, r_0, q_0, A_0

while a stationary point of E is not found

$k = k + 1$

$f_k = \arg\min_f E(f, r_{k-1}, q_{k-1}, A_{k-1})$

$r_k = \arg\min_r E(f_{k-1}, r, q_{k-1}, A_{k-1})$

$q_k = \arg\min_q E(f_{k-1}, r_{k-1}, q, A_{k-1})$

$A_k = \arg\min_A E(f_{k-1}, r_{k-1}, q_{k-1}, A)$

To solve the problem of minimization of the dual energy, which in general is not convex, a technique introduced by Blake and Zisserman can be used (see, e.g., [1, 2, 3, 5, 6, 11, 14, 15, 16, 17, 20]). With such a technique, called GNC (*Graduate Non-Convexity*), the energy function E, is approximated by means of a finite family $\{E^{(p)}\}$ of functions, in such a way that

the first one is convex and the last one coincides with the given function. Moreover, we call $\mathbf{x}$ the variable with respect to which we will compute the minimum of E. The algorithm is given as follows:

initialize $\mathbf{x}$

while $E_p \neq E$

find the minimum of the function E_p, starting with $\mathbf{x}$

replace $\mathbf{x}$ with the value found at the previous step

update the value of the parameter p

By choosing different approximating functions, it is possible to obtain various formulations of the GNC algorithm. The minimization of each of the approximating functions $E^{(p)}$ can be done by means of an algorithm called NL-SOR (*Non Linear Successive Over-Relaxation*) (see, e.g., [7]).

4 Determining the interference levels

In this paper, we deal with finding only the interference levels, fixed the recto, the verso and the blur mask. The other steps of the alternating algorithm will be treated in a forthcoming paper. The energy function with respect to the interference level is given by

$$\begin{aligned} & E(f_{k-1}, r_{k-1}, q, A_{k-1}) = \sum_{i=1}^{n}\sum_{j=1}^{m}\left(f^s(i,j) - f(i,j)\mathrm{e}^{-q_r(i,j)\left(1-\frac{z_r(i,j)}{N}\right)}\right)^2 + \\ + & \sum_{i=1}^{n}\sum_{j=1}^{m}\left(r^s(i,j) - r(i,j)\mathrm{e}^{-q_f(i,j)\left(1-\frac{z_f(i,j)}{N}\right)}\right)^2 + \\ + & S(q_f) + S(q_r) + S_c(q_f, q_r) + k, \end{aligned} \tag{4}$$

where k is a constant depending on f_{k-1} and r_{k-1}. Now, let

$$\psi(f) = r, \quad \psi(r) = f. \tag{5}$$

Given $v \in \{f, r\}$ and fixed a pixel (k, t), the partial derivative of the regularization terms with respect to $q_v(k, t)$ is

$$\begin{aligned}
&\frac{\partial(S(q_v) + S(q_{\psi(v)}) + S_c(q_v, q_{\psi(v)}))}{\partial q_v(k,t)} = \\
= \;& 2\lambda_v^2\Big(q_v(k,t) - q_v(k-1,t) + q_v(k,t) - q_v(k+1,t) + q_v(k,t) - q_v(k,t-1) + \\
+ \;& q_v(k,t) - q_v(k,t+1)\Big) + 2\lambda_c^2\Big(q_v(k,t) - q_{\psi(v)}(k,t)\Big) = \\
= \;& 2\lambda_v^2\Big(4q_v(k,t) - q_v(k-1,t) - q_v(k+1,t) - q_v(k,t-1) - q_v(k,t+1)\Big) + \\
+ \;& 2\lambda_c^2\Big(q_v(k,t) - q_{\psi(v)}(k,t)\Big).
\end{aligned}$$

Now we consider the Hessian matrix $\mathcal{H}$ related to the function $S(q_v) + S(q_{\psi(v)}) + S_c(q_v, q_{\psi(v)})$. Fix $v \in \{f, r\}$ and a pixel (k, t), on the associated row of $\mathcal{H}$, in correspondence with the principal diagonal we have

$$\frac{\partial^2(S(q_v) + S(q_{\psi(v)}) + S_c(q_v, q_{\psi(v)}))}{\partial q_v^2(k,t)} = 8\lambda_v^2 + 2\lambda_c^2,$$

and the non-null terms are given by

$$\frac{\partial^2(S(q_v) + S(q_{\psi(v)}) + S_c(q_v, q_{\psi(v)}))}{\partial q_v(k,t)\;\partial\,\eta} = -2\,\lambda_v^2,$$

where $\eta \in \{q_v(k-1,t),\, q_v(k+1,t),\, q_v(k,t-1),\, q_v(k,t+1)\}$, and

$$\frac{\partial^2(S(q_v) + S(q_{\psi(v)}) + S_c(q_v, q_{\psi(v)}))}{\partial q_v(k,t)\;\partial\, q_{\psi(v)}(k,t)} = -2\,\lambda_c^2.$$

Since λ_v and λ_c are different from zero, $\mathcal{H}$ is irreducible, and for $k = 1$ and $t = 1$ the variable η assumes only two values, then by virtue of the Gerschgorin theorems (see, e.g., [10]) the matrix $\mathcal{H}$ is positive-definite, and hence the sum of the smoothness terms is a convex function.

Now, fixed $v \in \{f, r\}$ and a pixel (k, t), let us consider the consistency term $T(q) = T_v(q_{\psi(v)}) + T_{\psi(v)}(q_v)$, related to the interference level of (4). We get:

$$\begin{aligned}
&\frac{\partial T(q)}{\partial q_v(k,t)} = \\
= \;& 2\Bigg((\psi(v))^s(k,t) - \psi(v)(k,t)e^{-q_v(k,t)\left(1-\frac{z_v(k,t)}{N}\right)}\Bigg)\psi(v)(k,t)e^{-q_v(k,t)\left(1-\frac{z_v(k,t)}{N}\right)}\left(1 - \frac{z_v(k,t)}{N}\right) = \\
= \;& 2\left(1 - \frac{z_v(k,t)}{N}\right)\psi(v)(k,t)\Bigg(\psi(v)^s(k,t)e^{-q_v(k,t)\left(1-\frac{z_v(k,t)}{N}\right)} - \psi(v)(k,t)e^{-2q_v(k,t)\left(1-\frac{z_v(k,t)}{N}\right)}\Bigg);
\end{aligned}$$

$$\frac{\partial^2 T(q)}{\partial q_v(k,t)^2} = 2\left(1-\frac{z_v(k,t)}{N}\right)^2 \psi(v)(k,t) \left(-(\psi(v))^s(k,t) e^{-q_v(k,t)\left(1-\frac{z_v(k,t)}{N}\right)} + 2\psi(v)(k,t) e^{-2q_v(k,t)\left(1-\frac{z_v(k,t)}{N}\right)} \right). \quad (6)$$

Since the second mixed derivatives are equal to zero, then the Hessian matrix is a diagonal matrix, whose elements are given in (6). Such elements are positive if and only if

$$q_v(k,t) < -\frac{\ln\left(\frac{(\psi(v))^s(k,t)}{2\,\psi(v)(k,t)}\right)}{1-\frac{z_v(k,t)}{N}} \quad \text{for all } v \in \{f,r\},\ k \in \{1,\dots,n\},\ t \in \{1,\dots,m\}.$$

Thus, the energy function related to the interference level is given by the sum of the terms of data consistency, which are not necessarily convex, and the smoothness terms, which are convex. Hence, in general the uniqueness of the global minimum is not guaranteed.

5 Convex approximation of the data consistency term

To approximate the term of faithfulness to the data, it is possible to approximate T_r and T_f separately. Moreover, we can approximate each term of the sum in (3) separately too. Fixed $i \in \{1,\dots,n\}$, $j \in \{1,\dots,m\}$ and $v \in \{f,r\}$, let ψ be as in (5), and denoting by $\alpha = \dfrac{\psi(v)(i,j)}{\psi(v^s)(i,j)}$, $\gamma = \dfrac{z_v(i,j)}{N} - 1$, $q = q_v(i,j)$, the term related to the faithfulness to the data can be expressed as

$$\begin{aligned} T(f,r,q,A) &= T_f(q_r) + T_r(q_f) = \sum_{i=1}^{n}\sum_{j=1}^{m}\left(f^s(i,j) - f(i,j)\mathrm{e}^{-q_r(i,j)\left(1-\frac{z_r(i,j)}{N}\right)}\right)^2 + \\ &+ \sum_{i=1}^{n}\sum_{j=1}^{m}\left(r^s(i,j) - r(i,j)\mathrm{e}^{-q_f(i,j)\left(1-\frac{z_f(i,j)}{N}\right)}\right)^2 = \quad (7) \\ &= \sum_{i=1}^{n}\sum_{j=1}^{m}\sum_{v\in\{f,r\}} \psi(v)^s(i,j)\,\varphi_{i,j,v}(q), \end{aligned}$$

where

$$\varphi_{i,j,v}(q) = \left(1-\alpha\, e^{q\gamma}\right)^2 = 1 - 2\alpha\, e^{q\gamma} + \alpha^2\, e^{2q\gamma}. \quad (8)$$

Therefore, to make the function $\varphi_{i,j,v}$ in (8) convex, we will proceed in several ways. In particular, in this paper we approximate the quantity

$$g_{i,j,v}(q) = e^{q\gamma} \quad (9)$$

by a line of the type $\tilde{g}(q) = \tilde{A}\,q + \tilde{B}$. So, the approximation of $\varphi_{i,j,v}(q)$ is given by $\tilde{\varphi}(q) = (1 - \alpha\tilde{A}\,q - \tilde{B})^2$, which is a convex function, since $\tilde{\varphi}''(q) = 2\,\alpha^2\,\tilde{A}^2$.

5.1 Interpolating approximation

Now we approximate $g_{i,j,v}(q)$ with the line $p^{(1)}_{i,j,v}(q)$ interpolating at the points $(3, e^{3\gamma})$ and $(0, 1)$. To compute the interpolating polynomial, we use the Lagrange method, obtaining

$$p^{(1)}_{i,j,v}(q) = L_0(q)\bar{y}_0 + L_1(q)\bar{y}_1,$$

where $L_0(q)$, $L_1(q)$ are the Lagrange polynomial bases defined by

$$L_0(q) = \frac{q - \bar{x}_1}{\bar{x}_0 - \bar{x}_1} = \frac{q}{3}$$

and

$$L_1(q) = \frac{q - \bar{x}_0}{\bar{x}_1 - \bar{x}_0} = -\frac{1}{3}(q - 3),$$

and so we get

$$p^{(1)}_{i,j,v}(q) = q\left(\frac{e^{3\gamma}}{3} - \frac{1}{3}\right) + 1.$$

Thus, the convex approximation of $\varphi_{i,j,v}(q)$ is given by

$$\varphi^{(1)}_{i,j,v}(q) = \left(1 - \alpha\, q\frac{e^{3\gamma} - 1}{3} - \alpha\right)^2. \tag{10}$$

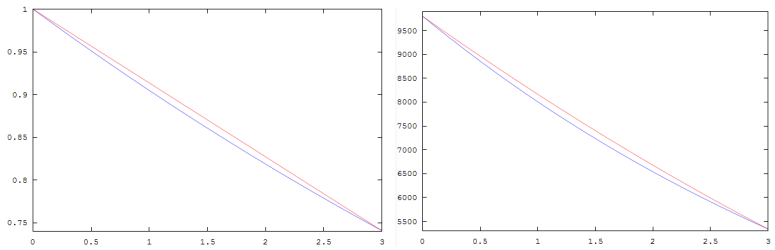

Figure 1: On the left side: Graph of $g_{i,j,v}(q)$ in blue and $p^{(1)}(q)$ in red. On the right side: Graph of $\varphi_{i,j,v}(q)$ in blue and $\varphi^{(1)}(q)$ in red ($\alpha = 100$, $\gamma = 0.1$).

5.2 The best line approximation

Now we approximate $g_{i,j,v}(q)$ by the line $p^{(2)}_{i,j,v}(q)$ of best approximation with respect to the 2-norm in $P_1([0,3]) = \{p : [0,3] \to \mathbb{R} |\ p \text{ is a polynomial of degree at most } 1\}$. We begin with using the Gram-Schmidt method to find an orthonormal basis $\{e_1, e_2\}$ for $P_1([0,3])$. We choose as basis the following polynomials:

$$x_1 = 1, \quad x_2 = q.$$

We normalize the first basis polynomial. We have

$$e_1 = \frac{x_1}{\|x_1\|} = \frac{1}{\sqrt{3}} = \frac{\sqrt{3}}{3}.$$

By applying the Gram-Schmidt algorithm, we get

$$z_2 = x_2 - < x_2, e_1 > e_1 = q_r - \frac{1}{3}\int_0^3 q\ dq = q - \frac{1}{3}\left[\frac{q^2}{2}\right]_0^3 = q - \frac{3}{2}.$$

By normalizing z_2 we obtain

$$e_2 = \frac{z_2}{\|z_2\|} = \frac{2}{3}\left(q - \frac{3}{2}\right),$$

where

$$\|z_2\| = \sqrt{\int_0^3 \left(q - \frac{3}{2}\right)^2 dq} = \frac{3}{2}.$$

So, we have constructed an orthonormal basis $\{e_1, e_2\}$ of $P_1([0,3])$. Thus, the best approximation polynomial of $g_{i,j,v}(q)$ is given by

$$p^{(3)}_{i,j,v}(q) = c_1 e_1 + c_2 e_2,$$

where

$$c_1 =< g_{i,j,v}, e_1 >= \int_0^3 g_{i,j,v}(q) e_1\ dq = \frac{\sqrt{3}}{3}\int_0^3 e^{q\gamma}\ dq = \frac{\sqrt{3}}{3}\left[\frac{e^{q\gamma}}{\gamma}\right]_0^3 = \frac{\sqrt{3}}{3}\frac{e^{3\gamma}}{\gamma} - \frac{\sqrt{3}}{3}\frac{1}{\gamma},$$

$$c_2 =< g, e_2 >= \int_0^3 g(q) e_2\ dq = \frac{2}{3}\int_0^3 e^{q\gamma}\left(q - \frac{3}{2}\right)\ dq = \frac{2}{3}\int_0^3 e^{q\gamma} q\ dq - \int_0^3 e^{q\gamma}\ dq =$$

$$= \frac{2}{3}\left\{\left[\frac{e^{q\gamma}}{\gamma} q\right]_0^3 - \int_0^3 \frac{e^{q\gamma}}{\gamma}\ dq\right\} - \left[\frac{e^{q\gamma}}{\gamma}\right]_0^3 =$$

$$= \frac{2}{3}\left\{3\frac{e^{3\gamma}}{\gamma} - \left[\frac{e^{q\gamma}}{\gamma^2}\right]_0^3\right\} - \frac{e^{3\gamma}}{\gamma} + \frac{1}{\gamma} = 2\frac{e^{3\gamma}}{\gamma} - \frac{2}{3}\frac{e^{3\gamma}}{\gamma^2} + \frac{2}{3}\frac{1}{\gamma^2} - \frac{e^{3\gamma}}{\gamma} + \frac{1}{\gamma}.$$

Thus, we have
$p^{(3)}_{i,j,v}(q) = c_1\, e_1(q) + c_2\, e_2(q) =$

$$= \frac{\sqrt{3}}{3}\left(\frac{\sqrt{3}}{3}\frac{e^{3\gamma}}{\gamma} - \frac{\sqrt{3}}{3}\frac{1}{\gamma}\right) + \frac{2}{3}\left(q - \frac{3}{2}\right)\left(2\frac{e^{3\gamma}}{\gamma} - \frac{2}{3}\frac{e^{3\gamma}}{\gamma^2} + \frac{2}{3}\frac{1}{\gamma^2} - \frac{e^{3\gamma}}{\gamma} + \frac{1}{\gamma}\right) =$$

$$= \frac{1}{3}\frac{e^{3\gamma}}{\gamma} - \frac{1}{3}\frac{1}{\gamma} + \frac{4}{3}\frac{e^3\gamma}{\gamma} q - \frac{4}{9}\frac{e^{3\gamma}}{\gamma^2} q + \frac{4}{9}\frac{1}{\gamma^2} q - \frac{2}{3}\frac{e^{3\gamma}}{\gamma} q + \frac{2}{3}\frac{1}{\gamma} q - 2\frac{e^{3\gamma}}{\gamma} + \frac{2}{3}\frac{e^{3\gamma}}{\gamma^2} - \frac{2}{3}\frac{1}{\gamma^2} + \frac{e^{3\gamma}}{\gamma} - \frac{1}{\gamma} =$$

$$= \frac{2}{3}\frac{1}{\gamma}\left(2e^{3\gamma} - \frac{2}{3}\frac{e^{3\gamma}}{\gamma} + \frac{2}{3}\frac{1}{\gamma} - e^{3\gamma} + 1\right) - \frac{5}{3}\frac{e^{3\gamma}}{\gamma} - \frac{4}{3}\frac{1}{\gamma} + \frac{2}{3}\frac{e^{3\gamma}}{\gamma^2} - \frac{2}{3}\frac{1}{\gamma^2} + \frac{e^{3\gamma}}{\gamma},$$

and hence we obtain $p^{(2)}_{i,j,v}(q) = A^{(2)}\, q + B^{(2)}$, where

$$\begin{aligned} A^{(2)} &= \frac{2}{3\,\gamma}\Big(2e^{3\gamma} - \frac{2(e^{3\gamma}-1)}{3\,\gamma} - e^{3\gamma} + 1\Big), \\ B^{(2)} &= -\frac{5\,e^{3\gamma}}{3\,\gamma} - \frac{4}{3\,\gamma} + \frac{2\,e^{3\gamma}}{3\,\gamma^2} - \frac{2}{3\,\gamma^2} + \frac{e^{3\gamma}}{\gamma}. \end{aligned}$$

The convex approximation of $\varphi_{i,j,v}(q)$ is

$$\varphi^{(2)}_{i,j,v}(q) = \Big(1 - \alpha\, A^{(2)}\, q - B^{(2)}\Big)^2. \tag{11}$$

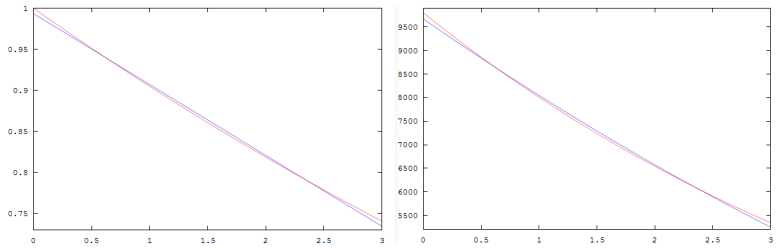

Figure 2: On the left side: Graph of $g_{i,j,v}(q)$ in blue and $p^{(2)}(q)$ in red. On the right side: Graph of $\varphi_{i,j,v}(q)$ in blue and $\varphi^{(2)}(q)$ in red ($\alpha = 100$, $\gamma = 0.1$).

5.3 Hybrid best approximation and interpolation

Now we approximate $g_{i,j,v}(q)$ by means of the line $p^{(5)}_{i,j,v}(q)$ of best approximation related to the 2-norm in $P_1([0,3]) = \{p : [0,3] \to \mathbb{R} |\ p$ is a polynomial of degree at most $1\}$, which interpolates $g_{i,j,v}(q)$ at a chosen point $\bar{q}$.
Now we make a change of coordinates, in such a way that the "new" origin coincides with $(\bar{q}, g_{i,j,v}(\bar{q}))$. Let us define

$$\tilde{g}(q) = g_{i,j,v}(q + \bar{q}) - g_{i,j,v}(\bar{q}). \tag{12}$$

Note that $\tilde{g}$ is a translation of $g_{i,j,v}$ in the Cartesian plane. Now we determine the polynomial $\tilde{p}^{(5)}$ of best approximation of $\tilde{g}$ with respect to the 2-norm in

$$P_1([-\bar{q}, 3-\bar{q}]) = \{p : [-\bar{q}, 3-\bar{q}] \to \mathbb{R} \mid p \text{ is a polynomial of degree at most } 1\}$$

which interpolates $\tilde{g}$ at 0.

We use the Gram-Schmidt method to find an orthonormal basis $\{e_1\}$ of the space

$$\{p \in P_1([-\bar{q}, 3-\bar{q}]) |\ p(0) = 0\}.$$

A basis for this space is given by $x_1 = q$. By normalizing, we get

$$||x_1|| = \sqrt{\int_{-\bar{q}}^{3-\bar{q}} q^2 \, dq} = \sqrt{3}\,(\sqrt{\bar{q}^2 - 3\bar{q} + 3}).$$

So, the normalized basis is given by

$$e_1 = \frac{x_1}{||x_1||} = \frac{q\sqrt{3}}{3(\sqrt{\bar{q}^2 - 3\bar{q} + 3})}.$$

The polynomial $\tilde{p}^{(5)}(q)$ of best approximation of $\tilde{g}_{i,j,v}(q)$ is

$$\tilde{p}^{(5)}(q) = c_1 e_1(q),$$

where

$$\begin{aligned} c_1 &= <\tilde{g}, e_1> = \int_{-\bar{q}}^{3-\bar{q}} \tilde{g}(q)\, e_1(q)\, dq = \\ &= -\frac{\sqrt{3}}{3(\sqrt{\bar{q}^2 - 3\bar{q} + 3})} e^{\bar{q}\gamma} \left(\frac{(\bar{q} - 3)e^{(3-\bar{q})\gamma} - \bar{q}\, e^{-\bar{q}\gamma}}{\gamma} + \frac{e^{(3-\bar{q})\gamma} - e^{-\bar{q}\gamma}}{\gamma^2} + \frac{9 - 6\bar{q}}{2} \right). \end{aligned}$$

Therefore, we get

$$\begin{aligned} \tilde{p}^{(5)}_{i,j,v}(q) &= -\frac{q}{6(\bar{q}^2 - 3\bar{q} + 3)} e^{\bar{q}\gamma} \left(\frac{(2\bar{q} - 6)e^{(3-\bar{q})\gamma} - 2\bar{q}\, e^{-\bar{q}\gamma}}{\gamma} + \right. \\ &+ \left. 2\frac{e^{(3-\bar{q})\gamma} - e^{-\bar{q}\gamma}}{\gamma^2} + 9 - 6\bar{q} \right). \end{aligned}$$

By taking the inverse translation, we obtain

$$p^{(5)}_{i,j,v}(q) = \tilde{p}^{(5)}(q - \bar{q}) + g_{i,j,v}(\bar{q}) = A^{(5)}(\bar{q})\, q + B^{(5)}(\bar{q}),$$

where

$$\begin{aligned} A^{(5)}(\bar{q}) &= -\frac{e^{\bar{q}\gamma}}{6(\bar{q}^2 - 3\bar{q} + 3)} \left(\frac{(2\bar{q} - 6)e^{(3-\bar{q})\gamma} - 2\bar{q}\, e^{-\bar{q}\gamma}}{\gamma} + \right. \\ &+ \left. 2\frac{e^{(3-\bar{q})\gamma} - e^{-\bar{q}\gamma}}{\gamma^2} + 9 - 6\bar{q} \right), \\ B^{(5)}(\bar{q}) &= \frac{\bar{q}\, e^{\bar{q}\gamma}}{6(\bar{q}^2 - 3\bar{q} + 3)} \left(\frac{(2\bar{q} - 6)e^{(3-\bar{q})\gamma} - 2\bar{q}\, e^{-\bar{q}\gamma}}{\gamma} + \right. \\ &+ \left. 2\frac{e^{(3-\bar{q})\gamma} - e^{-\bar{q}\gamma}}{\gamma^2} + 9 - 6\bar{q} \right) + e^{\bar{q}\gamma}. \end{aligned}$$

In particular, for $\bar{q} = 0$ we get

$$\begin{aligned} A^{(3)} &= A^{(5)}(0) = \frac{1}{18}\left(\frac{6e^{3\gamma}}{\gamma} - 2\frac{e^{3\gamma} - 1}{\gamma^2} - 9 \right), \\ B^{(3)} &= B^{(5)}(0) = \frac{1}{18}\, e^{3\gamma}\left(\frac{6e^{-3\gamma}}{\gamma} + 2\frac{e^{-3\gamma} - 1}{\gamma^2} + 9 \right), \end{aligned}$$

while for $\bar{q}$=3 we have

$$\begin{aligned} A^{(4)} &= A^{(5)}(3) = \frac{1}{18}\, e^{3\gamma}\left(\frac{6e^{-3\gamma}}{\gamma} + 2\frac{e^{-3\gamma}-1}{\gamma^2} + 9\right), \\ B^{(4)} &= B^{(5)}(3) = \frac{1}{6}\, e^{3\gamma}\left(\frac{6e^{-3\gamma}}{\gamma} + 2\frac{e^{-3\gamma}-1}{\gamma^2} + 9\right) + e^{3\gamma}. \end{aligned}$$

From this it follows that two possible convex approximation of $\varphi_{i,j,v}(q)$ are

$$\varphi^{(\kappa)}_{i,j,v}(q) = \left(1 - \alpha\, A^{(\kappa)}\, q - \alpha\, B^{(\kappa)}\right)^2, \quad \kappa = 3, 4. \tag{13}$$

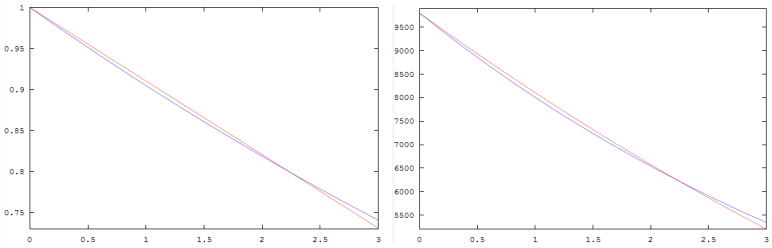

Figure 3: On the left side: Graph of $g_{i,j,v}(q)$ in blue and $p^{(3)}(q)$ in red. On the right side: Graph of $\varphi_{i,j,v}(q)$ in blue and $\varphi^{(3)}(q)$ in red ($\alpha = 100$, $\gamma = 0.1$).

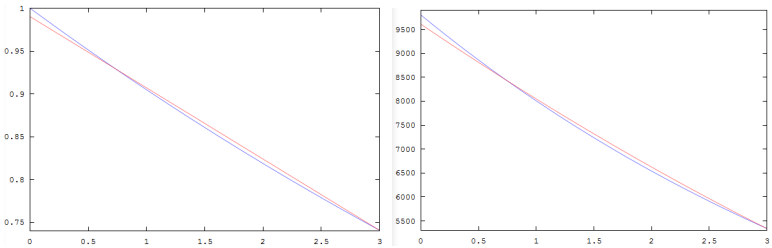

Figure 4: On the left side: Graph of $g_{i,j,v}(q)$ in blue and $p^{(4)}(q)$ in red. On the right side: Graph of $\varphi_{i,j,v}(q)$ in blue and $\varphi^{(4)}(q)$ in red ($\alpha = 100$, $\gamma = 0.1$).

6 The GNC approximation families

The first convex approximation of the consistency term of the energy function related to the interference level of the verso is expressed by

$$T^{(\kappa)}(f, r, q, A) = \sum_{i=1}^{n}\sum_{j=1}^{m}\sum_{v\in\{f,r\}} \psi(v)^s(i,j)\, \varphi^{(\kappa)}_{i,j,v}(q), \quad \kappa = 1, 2, 3, 4. \tag{14}$$

In this section, we define the following families of functions of convex approximations. Fixed $\kappa = 1, 2, 3, 4$, let

$$T^{(\kappa)}_p = p\, T^{(\kappa)} + (1-p)T.$$

For $p = 1$, we get the first convex approximation associated with κ, while for $p = 0$ we have the original function T.

7 Experimental results

In this section we compare the experimental results, by using the four different GNC algorithms proposed in the previous sections. We have assumed two different pairs of original images, given in Figures 5 and 6. We have used a uniform blur mask of dimension 5×5, and we have

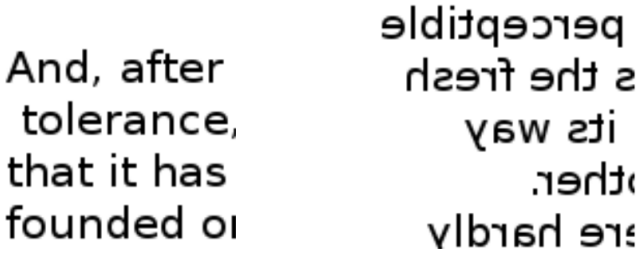

(a) (b)

Figure 5: First pair of ideal sources

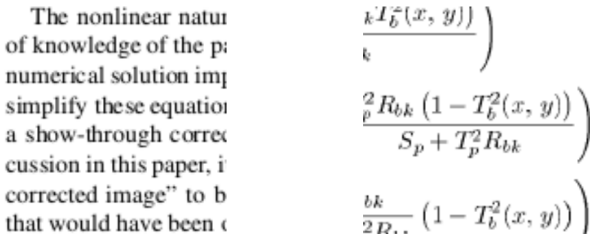

(a) (b)

Figure 6: Second pair of ideal sources

considered the interference levels to be estimated given in the Figure 7. In this figure, if the interference value of a single pixel is 0, that pixel is presented in black while, if the interference value is 3 (that is very high), then that pixel is presented in white. The gray pixels represent interference values between 0 and 3. Note that we have assumed that the ideal interference levels of the recto and of the verso coincide. Considering the first pair of original sources given in Figure 5 and the interference levels given by 7, we obtain the data mixtures given in Figure 8. We have tested the four GNC algorithms, assuming the following regularization parameters:

$$\lambda_f = \lambda_r = 50, \quad \lambda_c = 100.$$

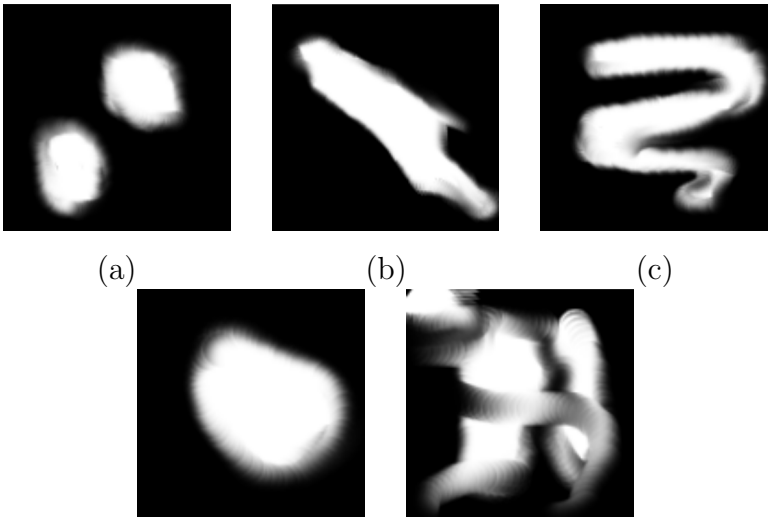

Figure 7: Interference levels: (a) $q_f^{(1)} = q_r^{(1)}$; (b) $q_f^{(2)} = q_r^{(2)}$; (c) $q_f^{(3)} = q_r^{(3)}$; (d) $q_f^{(4)} = q_r^{(4)}$; (e) $q_f^{(5)} = q_r^{(5)}$.

We have compared the four proposed algorithms in terms of mean square error (MSE) between the estimate of the obtained interference level and the ideal interference level given in Figure 7. In Table 1 the errors in terms of MSE obtained by the proposed algorithms, by considering the pair of original sources presented in Figure 5 and the interference levels $q_f^{(i)} = q_r^{(i)}$, $i = 1, \ldots, 5$, given in Figure 7. The effectiveness of the algorithm has been tested by using some images,

	$q_f^{(1)}$	$q_r^{(1)}$	$q_f^{(2)}$	$q_r^{(2)}$	$q_f^{(3)}$	$q_r^{(3)}$	$q_f^{(4)}$	$q_r^{(4)}$	$q_f^{(5)}$	$q_r^{(5)}$
$\kappa = 1$	0.05712	0.05332	0.07191	0.08313	0.07980	0.07843	0.08213	0.07920	0.10213	0.09871
$\kappa = 2$	0.03575	0.03741	0.03375	0.04121	0.04401	0.03979	0.03142	0.02673	0.03725	0.04165
$\kappa = 3$	0.03176	0.04002	0.03723	0.03937	0.04183	0.04272	0.02734	0.02639	0.04128	0.03984
$\kappa = 4$	0.02144	0.02347	0.02317	0.02242	0.03143	0.03031	0.00979	0.01127	0.03521	0.03878

Table 1: MSE of the proposed algorithms, using the original sources in Figure 5.

created to highlight the capacity of the algorithm to eliminate the degradations due to the effect of show-through.

As we see in Table 1, the best algorithm for the first pair of images is that related to the family of approximations with $\kappa = 4$. In Figure 9 there are the interference levels estimated by the algorithm corresponding with $\kappa = 4$.

Considering the second pair of original sources given in Figure 6 and the interference levels given by 7, and considering a uniform mask of type 5×5, we obtain the data mixtures given

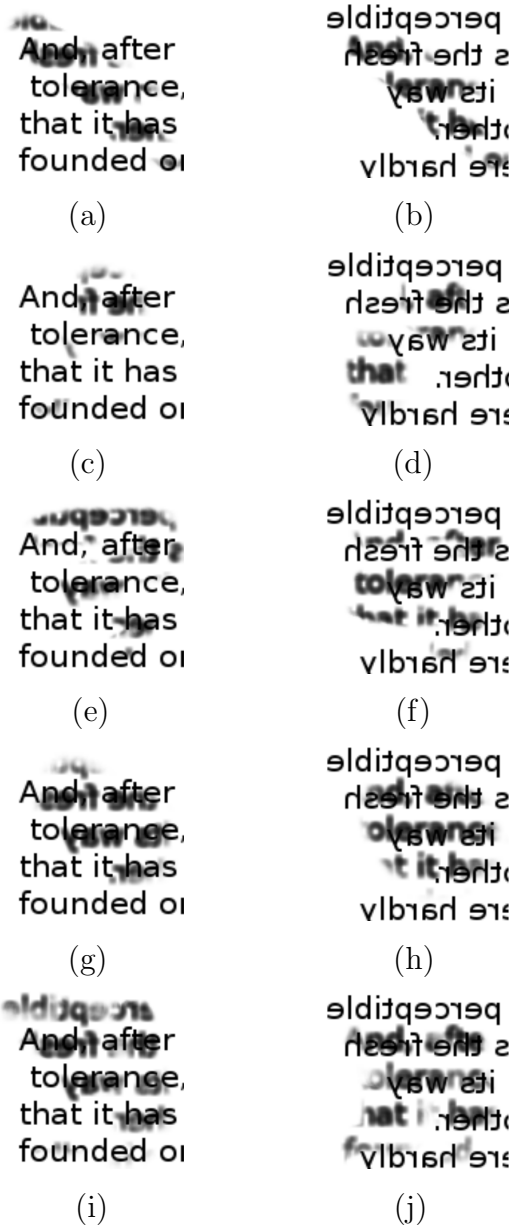

Figure 8: (a) Image in Figure 5 (a) with degraded by the interference level in Figure 7 (a); (b) image in Figure 5 (b) with degraded by the interference level in Figure 7 (a); (c) image in Figure 5 (a) with degraded by the interference level in Figure 7 (b); (d) image in Figure 5 (b) with degraded by the interference level in Figure 7 (b); (e) image in Figure 5 (a) with degraded by the interference level in Figure 7 (c); (f) image in Figure 5 (b) with degraded by the interference level in Figure 7 (c); (g) image in Figure 5 (a) with degraded by the interference level in Figure 7 (d); (h) image in Figure 5 (b) with degraded by the interference level in Figure 7 (d); (i) image in Figure 5 (a) with degraded by the interference level in Figure 7 (e); (j) image in Figure 5 (b) with degraded by the interference level in Figure 7 (e)

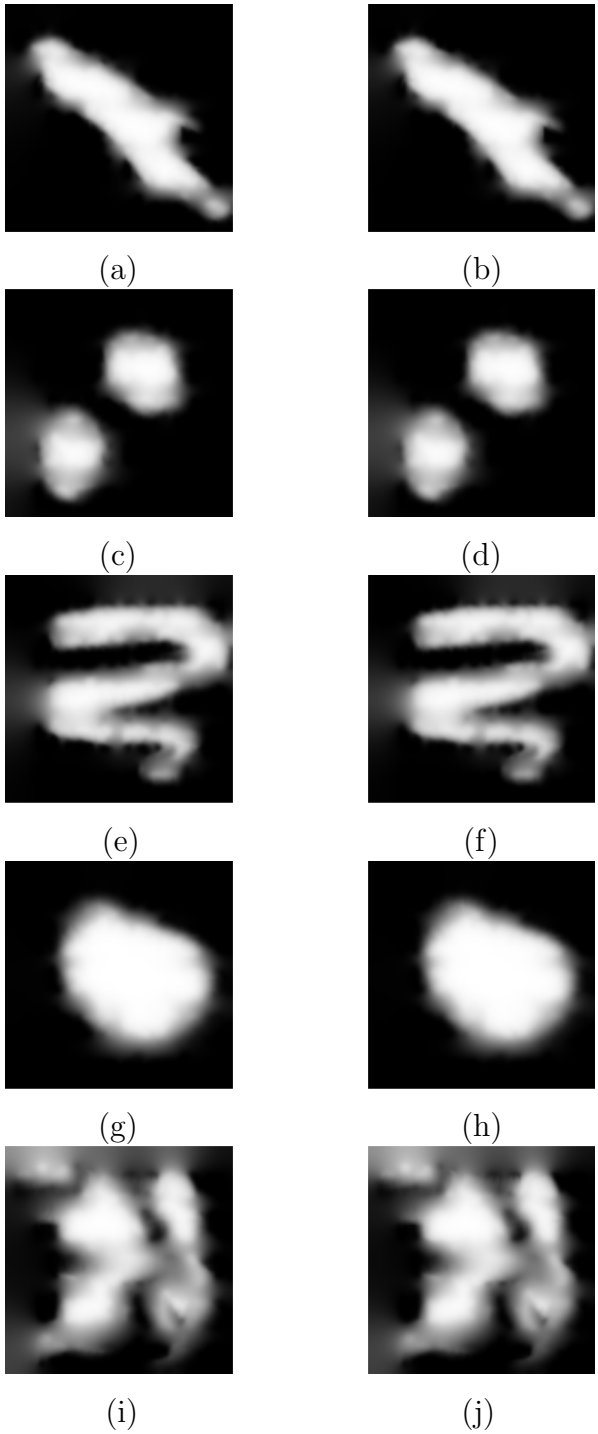

Figure 9: (a) estimation of $q_f^{(1)}$; (b) estimation of $q_r^{(1)}$; (c) estimation of $q_f^{(2)}$; (d) estimation of $q_r^{(2)}$; (e) estimation of $q_f^{(3)}$; (f) estimation of $q_r^{(3)}$; (g) estimation of $q_f^{(4)}$; (h) estimation of $q_r^{(4)}$; (i) estimation of $q_f^{(5)}$; (j) estimation of $q_r^{(5)}$.

in Figure 10. We have tested the four GNC algorithms, using the previous regularization parameters. In Table 2 the errors in terms of MSE obtained by the proposed algorithms, by considering the pair of original sources presented in Figure 6 and the interference levels $q_f^{(i)} = q_r^{(i)}$, $i = 1, \ldots, 5$, given in Figure 7.

	$q_f^{(1)}$	$q_r^{(1)}$	$q_f^{(2)}$	$q_r^{(2)}$	$q_f^{(3)}$	$q_r^{(3)}$	$q_f^{(4)}$	$q_r^{(4)}$	$q_f^{(5)}$	$q_r^{(5)}$
$\kappa = 1$	0.05229	0.04973	0.06127	0.06712	0.09415	0.08174	0.12176	0.13746	0.11288	0.15672
$\kappa = 2$	0.03374	0.03019	0.03626	0.03372	0.04791	0.03277	0.03711	0.04424	0.03845	0.04064
$\kappa = 3$	0.03147	0.03133	0.03317	0.03533	0.03179	0.03375	0.04176	0.05727	0.03973	0.03927
$\kappa = 4$	0.02379	0.02517	0.02433	0.02536	0.01017	0.01752	0.02578	0.03225	0.03320	0.03584

Table 2: MSE of the proposed algorithms, using the original sources in Figure 6.

As we see in Table 2, the best algorithm for the first pair of images is again that related to the family of approximations with $\kappa = 4$. In Figure 11 the interference levels estimated by the algorithm corresponding with $\kappa = 4$.

Conclusions

We have studied the problem of blind separation of the components, in particular concerning ancient documents corrupted by bleed-through and show-through. Thus, we have dealt with the problem of studying a regularization technique, which estimates the original sources, the interference levels and the blur operators. In this paper we have investigated the estimate of the interference levels, given the original sources and the blur operators. In particular, we have analyzed various GNC-type algorithms for minimizing the involved energy function. Such algorithms are different because of the choice of the first convex approximation. By means of the experimental results, we have determined which algorithm gives more accurated estimates of the interference levels.

References

[1] Bedini, L., Gerace, I., Tonazzini, A.: A Deterministic Algorithm for Reconstruction Images with Interacting Discontinuities. Computer Vision Graphics and Image Processing: Graphical Models Images Processing **56**, 109–123 (1994)

[2] Blake, A., Zisserman, A.: Visual Reconstruction. MIT Press, Cambridge, MA (1987)

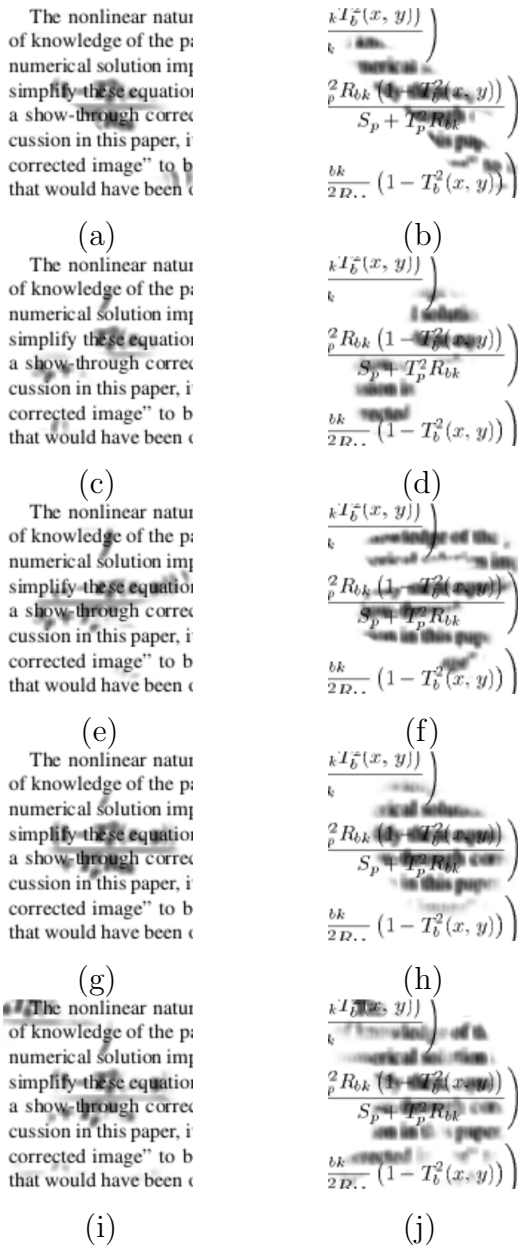

Figure 10: (a) Image in Figure 6 (a) with degraded by the interference level in Figure 7 (a); (b) image in Figure 6 (b) with degraded by the interference level in Figure 7 (a); (c) image in Figure 6 (a) with degraded by the interference level in Figure 7 (b); (d) image in Figure 6 (b) with degraded by the interference level in Figure 7 (b); (e) image in Figure 6 (a) with degraded by the interference level in Figure 7 (c); (f) image in Figure 6 (b) with degraded by the interference level in Figure 7 (c); (g) image in Figure 6 (a) with degraded by the interference level in Figure 7 (d); (h) image in Figure 6 (b) with degraded by the interference level in Figure 7 (d); (i) image in Figure 6 (a) with degraded by the interference level in Figure 7 (e); (j) image in Figure 6 (b) with degraded by the interference level in Figure 7 (e)

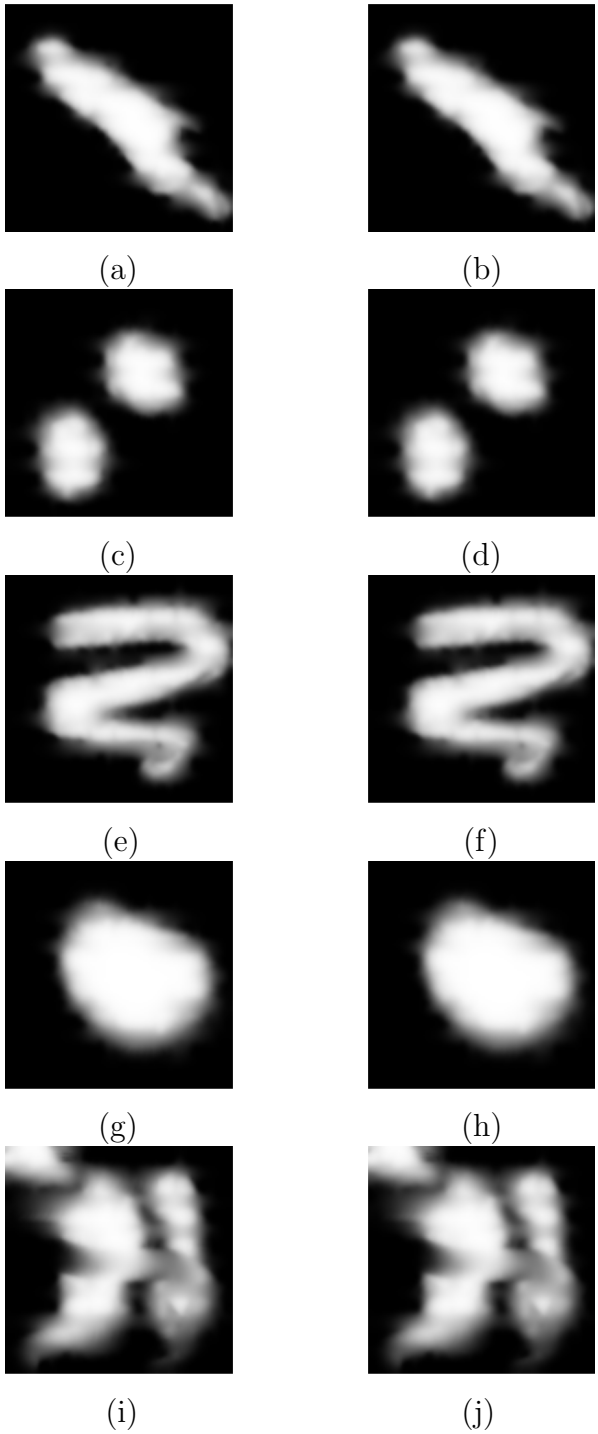

Figure 11: (a) estimation of $q_f^{(1)}$; (b) estimation of $q_r^{(1)}$; (c) estimation of $q_f^{(2)}$; (d) estimation of $q_r^{(2)}$; (e) estimation of $q_f^{(3)}$; (f) estimation of $q_r^{(3)}$; (g) estimation of $q_f^{(4)}$; (h) estimation of $q_r^{(4)}$; (i) estimation of $q_f^{(5)}$; (j) estimation of $q_r^{(5)}$.

[3] Boccuto, A., Gerace, I.: Image reconstruction with a non-parallelism constraint. In: Proceedings of the International Workshop on Computational Intelligence for Multimedia Understanding, Reggio Calabria, Italy, 27-28 October 2016, IEEE Conference Publications, pp. 1–5 (2016)

[4] Boccuto, A., Gerace, I., Giorgetti, V.: A Blind Source Separation Technique for Document Restoration. SIAM J. Imaging Sci. **12** (2), 1135–1162 (2019)

[5] Boccuto, A., Gerace, I., Martinelli, F.: Half-Quadratic Image Restoration with a Non-Parallelism Constraint. J. Math. Imaging Vision **59** (2), 270–295 (2017)

[6] Boccuto, A., Gerace, I., Pucci, P.: Convex Approximation Technique for Interacting Line Elements Deblurring: A New Approach. J. Math. Imaging Vision **44** (2), 168–184 (2012)

[7] Brewster, M. E., Kannan, R.: Nonlinear Successive Over-Relaxation. Numerische Math. **44** (2), 3019–3015 (1984)

[8] Gerace, I., Martinelli, F., Tonazzini, A.: Restoration of Recto-Verso Archival Documents Through a Regularized Nonlinear Model. In: Proceedings of 20th European Signal Processing Conference EUSIPCO, pp. 1588–1592 (2012)

[9] Gerace, I., Palomba, C., Tonazzini, A.: An inpainting technique based on regularization to remove bleed-through from ancient documents. In: 2016 International Workshop on Computational Intelligence for Multimedia Understanding (IWCIM), pp. 1–5 (2016)

[10] Gerschgorin, S.: Über die Abgrenzung der Eigenwerte einer Matrix. Izv. Akad. Nauk. USSR Otd. Fiz.-Mat. Nauk **6**, 749–754 (1931)

[11] Hazan, E., Levy, K. Y., Shalev-Shwartz, S.: On Graduated Optimization for Stochastic Non-Convex Problems. In: Proceedings of the 33 rd International Conference on Machine Learning, New York, NY, USA, 2016. JMLR: W& CP **48**, pp. 1–9 (2016)

[12] Khan, M. R., Imtiaz, H., Hasan, M. K.: Show-Through Correction in Scanned Images using Joint Histogram. Signal, Image and Video Processing **4** (3), 337–351 (2010)

[13] Martinelli, F., Salerno, E., Gerace, I., Tonazzini, A.: Nonlinear model and constrained ML for removing back–to–front interferences from recto–verso documents. Pattern Recognition **45**, 596–605 (2012)

[14] Mobahi, H., Fisher, J. W.: A Theoretical Analysis of Optimization by Gaussian Continuation. In: W.-K. Wong and D. Lowd (Eds.), Twenty–Ninth Conference on Artificial

Intelligence of the Association for the Advancement of Artificial Intelligence (AAAI), Proceedings. Austin, Texas, USA, January 25-30, 2015, pp. 1205–1211 (2015)

[15] Nikolova, M.: Markovian reconstruction using a GNC approach. IEEE Trans. Image Processing **8** (9), 1204–1220 (1999)

[16] Nikolova, M., Ng, M. K., Tam C.–P.: On ℓ_1 Data Fitting and Concave Regularization for Image Recovery. SIAM J. Sci. Comput., **35** (1), A397–A430 (2013)

[17] Nikolova, M., Ng, M. K., Zhang, S., Ching, W.-K.: Efficient Reconstruction of Piecewise Constant Images Using Nonsmooth Nonconvex Minimization. SIAM J. Imaging Sci. **1** (1), 2–25 (2008)

[18] Ophir, B., Malah, D.: Improved Cross-Talk Cancellation in Scanned Images by Adaptive Decorrelation. In: Proceedings of 23rd IEEE Convention of Electrical and Electronics Engineers in Israel, p. 4 (2004)

[19] Ophir, B., Malah, D.: Show-Through Cancellation in Scanned Images using Blind Source Separation Techniques. In: Proceedings of IEEE International Conference on Image Processing, (3) pp. 233–236 (2007)

[20] Robini, M. C., Magnin, I. E.: Optimization by Stochastic Continuation. SIAM J. Imaging Sci. **3** (4), 1096–1121 (2010)

[21] Salerno, E., Martinelli, F., Tonazzini, A.: Nonlinear Model Identification and See-Through Cancelation from Recto/Verso Data. International Journal on Document Analysis and Recognition (IJDAR) **16** (2), 177–187 (2013)

[22] Sharma, G.: Show-through cancellation in scans of duplex printed documents. IEEE Trans. on Image Processing **10**, 736–754 (2001)

[23] Tonazzini, A., Gerace, I., Martinelli, F.: Document Image Restoration and Analysis as Separation of Mixtures of Patterns: From Linear to Nonlinear Models. In: B. K. Gunturk and X. Li (Eds.), Image Restoration - Fundamentals and Advances, CRC Press, Taylor & Francis, Boca Raton, pp. 285–310 (2013)

[24] Tonazzini, A., Savino, P., Salerno, E.: A non-stationary density model to separate overlapped texts in degraded documents. SIViP **9** (Suppl. 1), S155–S164 (2015)